Desalination and Water Treatment
www.deswater.com
doi: 10.5004/dwt.2021.26598

212 (2021) 297–310
February

Separation of dye using surfactant as a collector in foam fractionation: modeling and optimization by response surface methodology and grey relational analysis

Tarun Kumar Bharadwaj, Kaushal Naresh Gupta*

Department of Chemical Engineering, Jaypee University of Engineering and Technology, A.B. Road, Raghogarh, Guna – 473226 (M.P.), India, Tel. +91-7544-267051; emails: kaushalnaresh74@gmail.com (K.N. Gupta), tarun.bharadwaj7@gmail.com (T.K. Bharadwaj)

Received 22 February 2020; Accepted 28 September 2020

ABSTRACT

The foam fractionation column was set up to enable the separation of methylene blue dye (MB) by utilizing sodium dodecyl sulfate (SDS) as a surfactant that serves as a collector. The effect of operating variables like SDS dosage, pH, air flow rate, liquid loading, and dye concentration was examined on percentage removal, enrichment ratio, and surface excess. Experiments were designed based on the Box–Behnken methodology. Response surface methodology was then implemented to investigate the interaction effects between the operating variables on response namely percentage removal and enrichment ratio. The accuracy of the mathematical model developed was asserted by higher values of the regression coefficient (0.962 for percentage removal and 0.969 for enrichment ratio). Further, the grey relational analysis tool was applied for the estimation of the optimum operating variable's values to obtain maximum percentage removal and enrichment ratio. The optimum values came out to be: air flow rate 150 mL min^{-1}; liquid loading 600 mL, and dye concentration 35 mL min^{-1}, respectively, at 95.8% removal with enrichment ratio of 7.7.

Keywords: Methylene blue; Sodium dodecyl sulfate; Percentage removal; Enrichment ratio; Optimization

1. Introduction

An upsurge in water pollution problems in the last few decades caused by the discharge of innumerable pollutants from various sources is a major area of concern for the researchers as it poses a threat to the environment, hence needs to be curbed forthwith. Undoubtedly, process industries are reported to be the major source of water pollution owing to the swift growth in industrial developments in recent times. One such industrial pollutant which has been persistently receiving the attention of the research community is dyeing wastewater. There are varieties of industries viz., textile, dyestuffs, paper, and plastics which play a vital role in the generation of colored wastewater because of the involvement of dyeing processes at different stages. It is reported in the literature that there are around 1,00,000 commercial dyes available with whopping 7,00,000 metric tons annual production worldwide [1]. Dyes are organic molecules comprising of complex aromatic structure which generally imparts color and makes them non-biodegradable [2–5]. This colored wastewater responsible for hampering the penetration of sunlight when discharged into water bodies causes substantial damage to the photosynthetic aquatic life [6–9].

In the present work, methylene blue (MB) employed for dyeing silk or cotton was adopted as a model dye. The harmful health effects of this dye include eye irritation, nausea, copious sweating, mental confusion, etc. [10]. The toxic nature of dyes thus necessitates its destruction/removal from the receiving water bodies by using an efficient and

* Corresponding author.

at the same time cost-effective technique. Several techniques for the treatment of dyeing wastewater reported in the literature are oxidation, membrane separation, coagulation–flocculation, adsorption, flotation, precipitation, aerobic, and anaerobic biological processes [11–13]. All these techniques face a serious limitation of secondary pollution [14] in terms of high sludge production, membrane fouling, and adsorbent regeneration despite their color removing abilities.

Over the years, foam fractionation has been proved to be one of the effective, ecological, low-cost, and environmentally friendly techniques for wastewater treatment especially for the removal of surfactants, proteins, and heavy metal ions. The other notable features that render foam fractionation a desirable separation process are (i) its ability to treat dilute solutions with reasonably good separation efficiency, (ii) no solvent is required, and (iii) can be operated both in continuous and batch-wise mode [15,16]. It is known as an adsorptive bubble separation technique where isolation of species is performed based on surface activity. It uses bubbles, generated by sparging gas at the bottom through the liquid column, thus concentrating surface-active species on the gas–liquid interface through preferential adsorption [17]. The bubbles then move up the solution and accumulate over the surface of the liquid to produce a foam phase containing a small quantity of entrained liquid between the bubbles. This entrained liquid tends to gravitate toward the bulk liquid solution resulting in dryer foam. Finally, the foam that emerges out of the column is collapsed and is referred to as foamate, is enriched with impurity. Dye removal using foam fractionation also requires a surfactant (collector) as dyes are not surface active and also do not generate foam when aerated. The dye-surfactant complex thus formed during their interaction gets adsorbed on the surface of the bubbles eventually leads to the separation of dye. Recently, this technique has also gained popularity in the field of dyeing wastewater treatment. However, there are only a few studies available on the dye removal in the literature using foam fractionation namely, methyl orange removal by using dodecyl dimethyl betaine as a collector [18], rhodamine B and cetyl trimethyl ammonium bromide removal by using sodium dodecylbenzene sulfonate as a collector [19], Direct black 17 removal by using cetyl trimethyl ammonium bromide as a collector [20], methylene blue removal using sodium dodecyl sulfate (SDS) as a collector [21], crystal violet removal by using SDS as a collector [22]. This study employed SDS, an anionic surfactant as a collector for the removal of cationic dye (MB). Enrichment ratio and percentage removal are the two important parameters used for evaluating the performance of any foam fractionation column. The key operating parameters which affect the efficiency of the foam fractionation column are air flow rate, liquid loading, dye concentration, surfactant dosage, and pH of the solution.

The present study also dealt with the optimization of these above stated operating variables with respect to enrichment ratio and percentage removal for an in-depth understanding of the foam separation technique. Before this, the response surface methodology (RSM) technique was employed for mathematical modeling to enable prediction of response at different operating conditions. Also, this technique assumes significance in investigating the effects of interaction between the variables on the response. Experiments are usually designed by employing the techniques namely central composite design (CCD) and Box–Behnken design (BBD). BBD yields a lesser number of experiments which makes it more attractive in comparison to CCD. This technique has widespread applications in the various areas of chemical engineering viz. adsorption, leaching, electrocoagulation, extraction, etc., enables to predict the response and optimized conditions for getting the desired response [23–26]. BBD technique was hence employed in this study for the design of experiments. Multi-objective optimization was finally carried out to ascertain the optimum conditions for obtaining higher enrichment ratio and percentage removal simultaneously. This was accomplished by using grey relational analysis (GRA) technique.

The objectives of this study are: (i) to conduct foam fractionation experiments for the isolation of MB using SDS at varying operating conditions namely pH, SDS concentration, airflow rate, feed dye concentration, and liquid loading to investigate the effect on percentage removal, enrichment ratio, and surface excess, (ii) to develop a mathematical model using RSM with the help of BBD, (iii) optimization of operating variables to simultaneously maximize both enrichment ratio and percentage removal by applying a GRA technique.

2. Materials and methods

2.1. Chemicals and analytical methods

All the analytical grade chemicals were used. Methylene blue (MB) and SDS were procured from Merck Chemicals Ltd., Mumbai, India, and used as it is without any further treatment. All the experiments were conducted by employing distilled water. The concentration of MB in SDS was found out by the UV-vis spectrophotometer (Elico SL210 double beam) at the greatest absorption wavelength of 610 nm.

2.2. Equipment

A schematic representation of the experimental batch foam fractionation column employed in this work is illustrated in Fig. 1. It was a cylindrical glass column of 1.1 m height and 0.05 m internal diameter. The column was provided with two inlet points to avoid any damage to the sparger during the filling of a liquid solution into the column. A sintered glass filter having 100–160 μm mean pore diameter was used as an air sparger, installed at the bottom of the column. The compressor was used to supply air through the sparger.

2.3. Experimental procedure

At the beginning of each run, the column was filled with a known concentration and known volume of feed solution (dye + surfactant). Then the pressurized air at a measured volumetric flow rate was introduced through a sintered glass diffuser installed near the base of the column

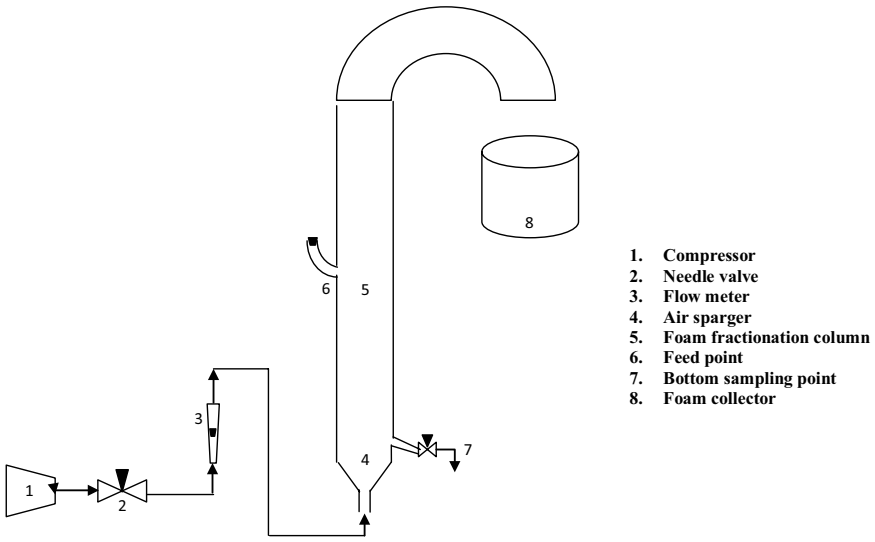

Fig. 1. Schematic diagram of the experimental set-up for foam fractionation.

to generate bubbles that rose to form foam above the liquid surface. The column was operated at room temperature (25°C ± 2°C). After the designated time interval, samples of foam leaving the top of the column through foam draw-off, and the residual liquid solution left in the column were collected. The foam samples were kept for some time to obtain collapsed foam. The samples were then analyzed to estimate the dye concentration using spectrophotometry.

2.4. Parameters estimation

In this section parameters required for the analysis of foam fractionation column along with their expressions have been mentioned.

2.4.1. Separation efficiency

The performance of the foam fractionation column in removing the dye from a liquid solution was estimated by evaluating these two parameters: enrichment ratio and percentage recovery.

Enrichment ratio (E) is the ratio of the concentration of dye in the foam phase to the dye concentration in the initial solution, given by:

$$E = \frac{C_f}{C_i} \tag{1}$$

where C_i (mg L^{-1}) and C_f (mg L^{-1}) are the dye concentrations in the feed solution and foamate (collapsed foam solution), respectively.

Percentage removal (R) is expressed as the percentage decrease in dye concentration relative to the initial dye concentration of the liquid solution.

$$R = \left(\frac{C_i - C_e}{C_i}\right) \times 100 \tag{2}$$

where C_e (mg L^{-1}) is the concentration of dye in the residual liquid solution.

2.4.2. Foam wetness

Foam exiting the column comprises of both liquid and air bubbles (i.e., gas). Volume fraction occupied by the liquid in the exiting foam phase (liquid hold up) is an important term in determining the wetness of the foam which in turn affects the separation efficiency. Hence, foam liquid hold up at the exit of the column, $\in_{exit}$, was found out by:

$$\in_{\text{exit}} = \frac{V_f}{V_f + V_g} \tag{3}$$

where V_g (L) is the air volume admitted at the base of the column by the air compressor in a given time and where V_f (L) is the foamate volume accumulated in a given time.

2.4.3. Bubble size measurement

The determination of bubble diameter is required in estimating the interfacial surface area of the bubbles where adsorption takes place. For this purpose, bubble size distribution was found out by adopting a photographic technique whereby bubbles were photographed in the column with the help of a digital camera (Nikon Coolpix P600). For each experiment, around 100–200 bubbles were captured in each image whose mean bubble diameter was evaluated by using image analysis software ImageJ. Sauter's mean diameter (d_{32}) was employed as a measure of bubble size by assuming bubbles to be spherical throughout, expressed as:

$$d_{32} = \frac{\sum_{i=1}^{n} d_i^3}{\sum_{i=1}^{n} d_i^2} \tag{4}$$

where d_i is the ith bubble diameter and n is the total bubbles in each image d_{32}, thus computed was utilized to estimate the bubble specific interfacial area and hence surface excess, discussed in the succeeding section.

2.4.4. Determination of surface excess

Surface excess is a crucial parameter in assessing the amount of interfacial adsorption occurring on the surface of the bubbles hence providing insight into the foam fractionation phenomena. It is obtained by dividing the amount of dye adsorbed with the bubble surface area given by Eq. (5). Here, it was assumed that the concentration of dye in the entrained liquid of the foam was identical with the dye concentration in the bubbly liquid phase.

$$\Gamma = \frac{M}{A_0} \tag{5}$$

where Γ (mg m^{-2}) is known as surface excess, M the amount adsorbed (mg) onto bubble surface in a given time, and A_0 (m^2) the interfacial surface area of the bubbles, can be found out by using the following expression:

$$A_0 = \frac{0.006V_g}{d_{32}} \tag{6}$$

Now the adsorption of dye on the bubble surface can be estimated from the following expression:

$$M = \left(C_f - C_e\right)V_f \tag{7}$$

Finally, combining all the above equations, that is, Eqs. (5)–(7), we obtain:

$$\Gamma = \frac{\left(C_f - C_e\right)V_f d_{32}}{0.006V_g} \tag{8}$$

2.5. Experimental results

The experimental results acquired by performing the experiments at varying operating conditions have been discussed in detail in this section. Foam fractionation column in all the experiments was run for a fixed duration (25 min).

2.5.1. Effect of SDS concentration

The SDS dose was optimized by investigating the SDS concentration effect on the separation of MB dye. The surfactant concentration was found to have a profound effect on the separation efficiency of the column. The column was operated by varying the SDS concentration in the range of 250–2,000 ppm. The upper limit of 2,000 ppm for SDS was fixed based on the critical micelle concentration (CMC) of surfactant which is around 2,500 ppm as it is well-established that prior to CMC, surfactant exhibit poor adsorptive capacity as well as experience a substantial reduction in surface tension [21]. Consequently, the influence of SDS concentration was investigated until 2,000 ppm. The other operating variables such as the volumetric flow rate of air, liquid loading, and dye concentration were maintained constant at 200 mL min^{-1}, 750 mL, and 15 ppm, respectively in all the runs. The SDS concentration effect on enrichment ratio and percentage removal shown in Fig. 2 demonstrates the drop in enrichment ratio with an increase in SDS concentration. It may be attributed to the fact that at greater surfactant concentration, the surface tension of the liquid solution gets lowered, and also it becomes more viscous. Both these factors favored higher liquid fraction in the foam phase owing to the difficulty in releasing the interstitial liquid (film drainage). Finally, the wet foam generated from the top of the column with an increase in surfactant concentration had successively lower values of enrichment ratio. The percentage removal on the other hand (Fig. 2) was found to increase initially from 66% to 83% and finally decreasing with the rise in surfactant concentration. The initial increase in the percentage removal with SDS concentration (up to 700 ppm) may be due to the higher entrainment of the liquid following which bubble surface got saturated with the adsorbed surfactant and the excess surfactant added thereafter would compete for the vacant space on the air–bubble interface with the formed complexes which led to the decrease in percentage removal. These results were found to be consistent with the earlier study reported in the literature [21]. Eventually, the optimized SDS dosage was determined from Fig. 2 came out to be 500 ppm. All the dye removal experiments were then subsequently performed at 500 ppm SDS concentration.

2.5.2. Effect of initial pH

Initial pH of the feed solution is another significant parameter which affects dye separation due to varying concentration of H^+ and OH^- ions. Its effect on enrichment ratio and removal fraction was investigated by carrying out foam fractionation experiments at 15 ppm dye concentration, 750 mL liquid loading, 500 ppm SDS concentration, and 200 mL min^{-1} air flow rate, is illustrated in Fig. 3. The initial pH was varied in the range of 3–10 and was maintained by adding 0.5 N HCl and 0.5 N NaOH to the solution fed. Fig. 3 depicts the increasing trend for percentage removal followed by a decreasing trend with a rise in initial pH of the solution, while initial pH doesn't have any significant effect on enrichment ratio (7.1–7.25). In low pH range (high acidic conditions) the H^+ ions competed with the cationic dye thus making difficult the formation of a dye-surfactant aggregate resulting in a decrease in percentage removal. This may also be explained by the fact that the low pH of a solution engendered relatively poor foam stability and foam quality, causing a decrease in removal fraction. Similarly, at higher pH (alkaline conditions) presence of a higher concentration of OH^- ions made the formation of dye-surfactant complex tougher due to competition of OH^- ions with the anionic surfactant which finally led to the lowering of percentage removal. Also, at higher pH, strong alkalinity might have induced large water content in the foam phase which was responsible for the reduction in percentage removal. From Fig. 3 highest percentage removal was obtained at pH in the range

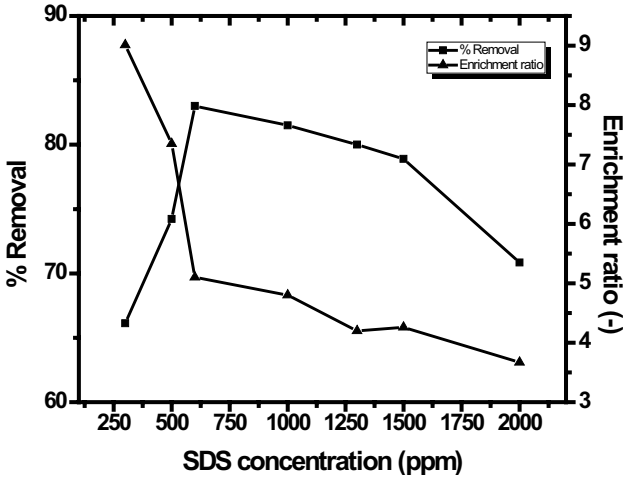

Fig. 2. Effect of SDS concentration on percentage removal and enrichment ratio (air flow rate = 200 mL min^{-1}, liquid loading = 750 mL, and dye concentration = 15 ppm).

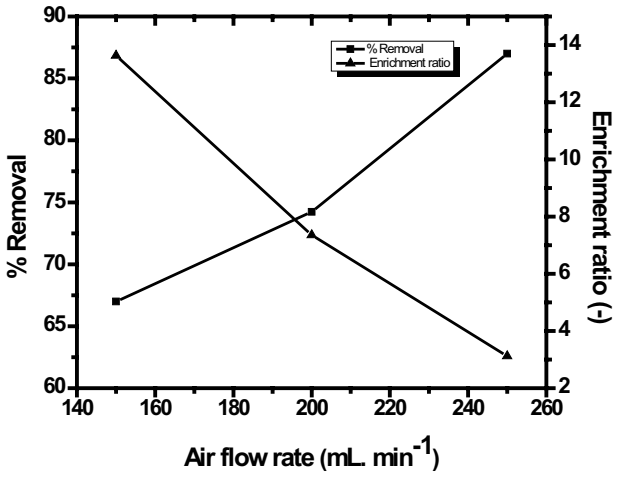

Fig. 4. Effect of air flow rate on percentage removal and enrichment ratio (liquid loading = 750 mL, dye concentration = 15 ppm, and SDS concentration = 500 ppm).

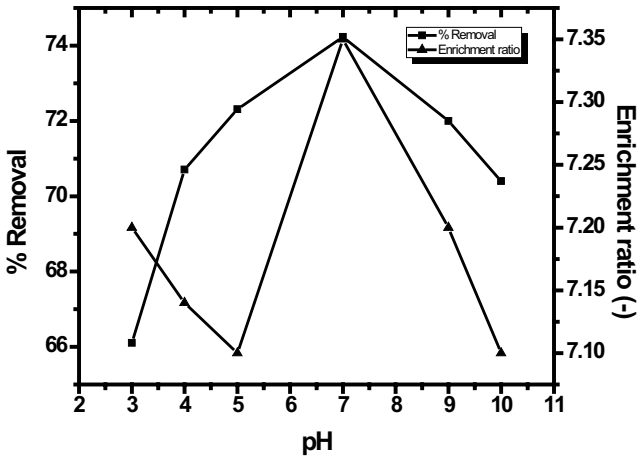

Fig. 3. Effect of initial pH on percentage removal and enrichment ratio (air flow rate = 200 mL min^{-1}, liquid loading = 750 mL, dye concentration = 15 ppm, and SDS concentration = 500 ppm).

of 6.5 to 7.5. Hence in this way, the initial pH of a solution was optimized and maintained at around 7 for investigating the effect of other variables in the present study.

2.5.3. Effect of airflow rate

The aeration rate has a significant role in the removal of dye in a foam fractionation column as it greatly affects the number of bubbles along with its foam phase residence time and foam production rate. The following operating conditions were employed to examine the effect of the flow rate of air on the performance of foam fractionation column: 15 ppm dye concentration, 750 mL liquid loading volume, and 500 ppm surfactant concentration. The volumetric flow rate of air was varied in 150–250 mL min^{-1} range and its effect on enrichment ratio and percentage removal is depicted in Fig. 4. It is evident from Fig. 4 that enrichment ratio declined whereas percentage removal rose with the increase in aeration rate. Higher flow rates generated a larger amount of gas bubbles as well as higher surface flux, which led to greater adsorption of dye-surfactant aggregate onto the surface of the bubble which eventually resulted in higher percentage removal. At the same time enrichment ratio decreased with an increase in air flow rate because of higher foam phase liquid hold up. This may be because higher gas flow rates caused shorter bubbles residence time in the foam phase thus getting lesser time for the foam drainage, hence more carryover of liquid and disengagement of wet foam from the top of the column. On the other hand at lower gas flow rates, the drier foam was obtained owing to greater bubbles residence time in the foam phase resulting in effective and enhanced foam drainage.

Surface excess (Fig. 5) was found to decrease at higher flow rates of air. Greater foamate concentration obtained at lower airflow rates was the main controlling factor in determining the value of surface excess which outweighed the increase in the surface area generated at higher aeration rates.

2.5.4. Effect of liquid loading

Liquid loading is also an important parameter in the removal of dye in foam fractionation studies with respect to residence time in liquid solution as well as in the foam phase. The effect of liquid loading on separation parameters (Fig. 6) was investigated by performing the experiments at 15 ppm initial dye concentration, 200 mL min^{-1} air flow rate, and 500 ppm surfactant concentration in the range of 600–900 mL liquid loading. The percentage removal decreased from 86% to 67.93% on varying the liquid loading from 600 to 900 mL. This decreasing trend may be explained by considering two factors operating simultaneously in deciding the value of percentage removal, that is, amount of dye in the feed and bubbles residence time in the solution. At higher liquid loading the mass of dye present would be more and the residence time of the bubbles in the solution would also be greater. But there would be a marginal increase in the residence time due to

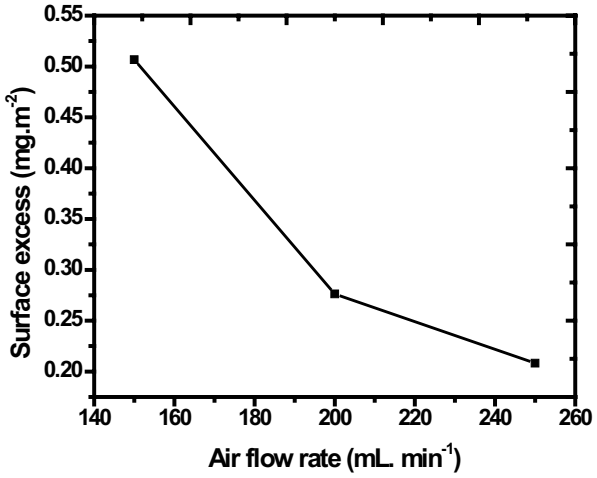

Fig. 5. Effect of air flow rate on surface excess (liquid loading = 750 mL, dye concentration = 15 ppm, and SDS concentration = 500 ppm).

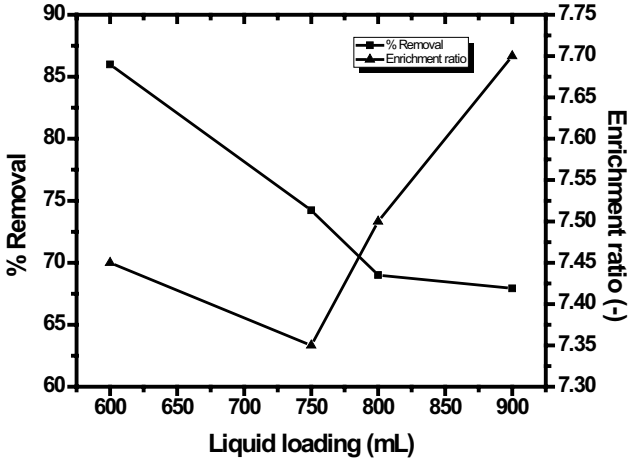

Fig. 6. Effect of liquid loading on percentage removal and enrichment ratio (air flow rate = 200 mL min^{-1}, dye concentration = 15 ppm, and SDS concentration = 500 ppm).

the increase in liquid loading resulting in an inconsiderable rise in the uptake of the dye by the bubbles. Owing to which the amount of dye (in mg) left in the residual solution would be higher at higher liquid loading, leading to higher dye concentration in the residual solution, hence lower percentage removal. In short, it can be said that the additional residence time provided by the increase in liquid loading was not enough to effect the increase in percentage removal of the dye. On the other hand, a slight increase in enrichment ratio was observed (Fig. 6) from 7.45 to 7.7 on increasing the liquid loading. Although the time provided for the foam drainage would be lesser at higher liquid loadings, the enrichment ratio marginally increased because of a higher concentration of dye in the interstitial liquid.

From Fig. 7 surface excess was found to be increasing with the increase in liquid loading. It may be attributed to the fact that higher foamate volume collected at higher

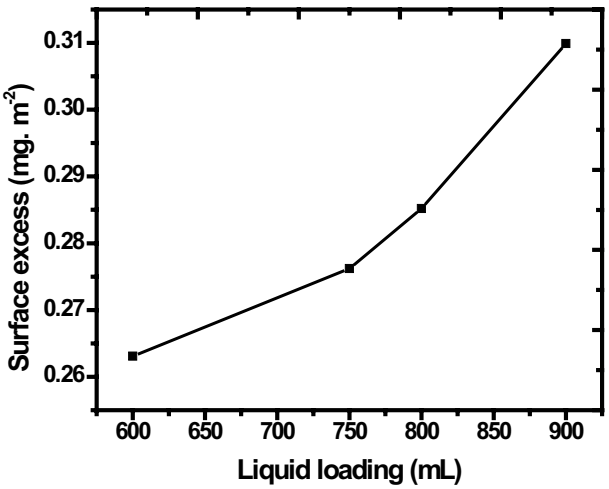

Fig. 7. Effect of liquid loading on surface excess (air flow rate = 200 mL min^{-1}, dye concentration = 15 ppm, and SDS concentration = 500 ppm).

liquid loading caused more amount of dye adsorption onto the bubble surface despite marginal variation in the foamate concentration, finally resulting in a rise in surface excess.

2.5.5. Effect of dye concentration

The initial dye concentration in the liquid solution was found to have an appreciable effect on the performance of a foam fractionation column. Its effect was investigated (Fig. 8) by changing the dye concentration in 5–25 ppm range by keeping other parameters such as aeration rate, liquid loading, and surfactant concentration constant at 200 mL min^{-1}, 750 mL, and 500 ppm, respectively. Percentage removal was found to decrease from 90% to 63% on increasing the concentration of dye from 5 to 25 ppm. It may be due to the same contact time (25 min) provided in all the experimental runs caused a lesser amount of dye to be removed at higher concentrations. As observed from Fig. 8, enrichment ratio fell from 8 to 3.9 on increasing the dye concentration from 10 to 25 ppm with an anomalous behavior at 5 ppm where enrichment ratio was found to be 4.1. The decrease in enrichment ratio occurred due to the higher viscosity of liquid entrapped between the bubbles at higher dye concentrations leading to lesser foam drainage. This is also evident from the higher values of $\in_{exit}$ (0.02534) obtained for 25 ppm dye concentration relative to 0.0172 at 10 ppm dye concentration. The lower value of enrichment ratio (4.1) at 5 ppm dye concentration was attributed to the fact that most of the dye got removed after 25 min resulting in lesser dye concentration in the foamate, hence lower enrichment ratio. It was also seen during the experiments that the color of the foam exiting the column at 5 ppm initial dye concentration was almost white indicating a lesser amount of dye present in the foam.

Surface excess was also evaluated, illustrated in Fig. 9, found to increase from 0.042 to 0.395 mg m^{-2} by increasing the dye concentration from 5 to 20 ppm. This may be due

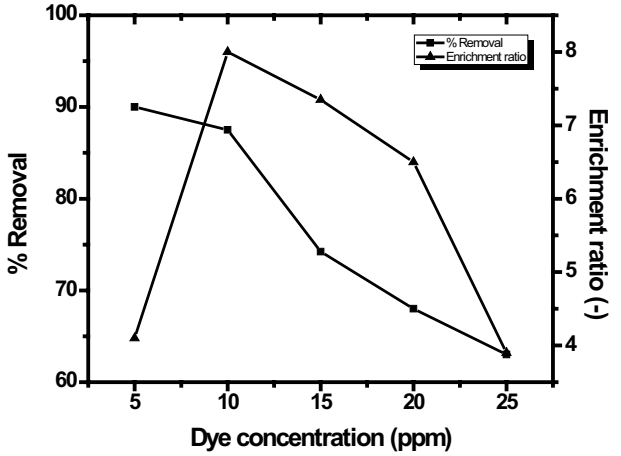

Fig. 8. Effect of dye concentration on percentage removal and enrichment ratio (air flow rate = 200 mL min^{-1}, Liquid loading = 750 mL, and SDS concentration = 500 ppm).

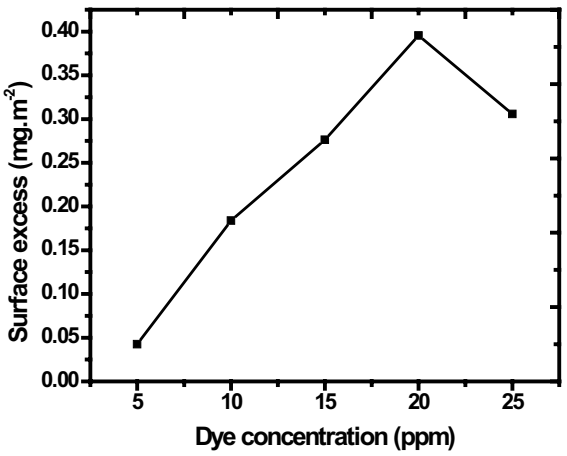

Fig. 9. Effect of dye concentration on surface excess (air flow rate = 200 mL min^{-1}, liquid loading = 750 mL, and SDS concentration = 500 ppm).

to the increase in foamate concentration at higher dye concentrations. At 25 ppm, the value of surface excess decreased to 0.306 mg m^{-2} because of a higher percentage reduction in enrichment ratio relative to 20 ppm. Also, the extremely low value of surface excess at 5 ppm dye concentration was due to the same reason stated in the preceding paragraph.

2.6. Experimental design

The effect of various operating variables can be investigated by using the technique of experimental modeling, useful for providing important insights into the process. Nowadays RSM is implemented to envisage the response of the process [27]. For this purpose, the relationship between controllable (input variables) parameters and response (output variable) was established in the form of a mathematical equation. Experimental data is required for obtaining a relationship between cause and effect which can be generated by employing the design of experiments. Here, the BBD technique has been implemented for designing the experiments. The operating variables which will likely influence percentage removal and enrichment ratio were identified as airflow rate (X_1), liquid loading (X_2), and dye concentration (X_3). The levels selected for these three operating variables are listed in Table 1. Following second-order polynomial was employed to develop an empirical relationship between response, Y, and input variables (X_i) [28]:

$$Y = \beta_0 + \sum_{i=1}^{n}\beta_i X_i + \sum_{i=1}^{n}\beta_{ii} X_i^2 + \sum_{i=1}^{n}\sum_{j=1}^{n}\beta_{ij} X_i X_j + \in \quad (9)$$

where Y is the response (percentage removal and enrichment ratio); β_0, β_i, β_{ii}, and β_{ij} are known as model coefficients; n and $\in$ are the number of pattern and error, respectively; input parameters are defined by X_i and X_j. BBD utilizes the following expression for the estimation of several experiments (N) required to be conducted for the response surface design [29]:

$$N = 2P\left(P-1\right) + X \quad (10)$$

Here, N = 15 for three factors and central points each, that is, P and X.

The design matrix was created by employing Minitab 14 software for the evaluation of response from Eq. (1). Foam fractionation experiments were performed for MB removal using SDS as a surfactant to estimate percentage removal and enrichment ratio under varying operating conditions like volumetric flow rate of air (150–250 mL min^{-1}), liquid loading (600–900 mL), and dye concentration (5–25 ppm). Table 2 presents the response of 15 sets of experiments given by BBD. Mathematical models deduced from the experimental results as a function of coded input variables for the prediction of response (Y) are as follows:

$$\begin{aligned} Y\left(\%\text{Removal}\right) &= 75.42 + 8.75X_1 - 7.825X_2 - 12.84X_3 \\ &+ 2.115X_1^2 - 1.645X_2^2 + 2.405X_3^2 + 2.57X_1X_2 + 4.34X_1X_3 \\ &- 4.43X_2X_3 \end{aligned} \quad (11)$$

$$\begin{aligned} Y\left(\text{Enrichment ratio}\right) &= 7.45 - 4.0825X_1 + 0.023X_2 + 0.0655X_3 \\ &+ 1.02575X_1^2 + 0.26925X_2^2 - 3.70075X_3^2 - 0.21X_1X_2 \\ &+ 0.16X_1X_3 + 0.0285X_2X_3 \end{aligned} \quad (12)$$

2.7. ANOVA interpretation

Further, the acceptability of developed models was confirmed by applying analysis of variance (ANOVA). Table 3 presents the ANOVA results for both percentage removal and enrichment ratio at a confidence interval of 95%. Lower values of P (<0.05) for both percentage removal and enrichment ratio demonstrated the significance of the developed models. Besides, higher values of R^2 obtained from Fig. 10 (0.962) and Fig. 11 (0.969) indicated satisfactory agreement between model and experimental response for both percentage removal and enrichment ratio. It may also be concluded from Table 3 that the linear effect of parameters in case of

percentage removal whereas both linear and square effect of parameters for enrichment ratio is significant in comparison to other effects.

2.7.1. Interaction effects of liquid loading and dye concentration

Fig. 12 demonstrates the interaction effect of liquid loading and dye concentration on percentage removal at a constant airflow rate of 200 mL min^{-1}. The decreasing trend in percentage removal was observed with the increase in liquid loading at different values of dye concentration. Similarly, the trend can be seen with the increase in dye concentration at different liquid loadings. In both cases, the percentage decrease in response increased at higher values of dye concentration and liquid loading. Fig. 12 also indicates that lower liquid loading and dye concentration is favorable to obtain higher percentage removal.

It may be observed from the response surface plot that lower values of both liquid loading and dye concentration are favorable to obtain higher values of the response.

Similarly, Fig. 13 shows the combined effects of these variables on the second response (enrichment) at 200 mL min^{-1} air flow rate. The liquid loading effect on the response at all dye concentrations was found to be almost negligible. The peculiar behavior was observed in case of variation in response with dye concentration at different liquid loadings. Enrichment was found to be minimum at lowest dye concentration, rose and then dropped with dye concentration at all liquid loadings. Hence, higher values of enrichment were favored at intermediate dye concentrations.

2.7.2. Interaction effects of airflow rate and liquid loading

Fig. 14 illustrates the interaction effects of aeration rate and liquid loading on percentage removal at 15 ppm inlet dye concentration. The response surface plot (Fig. 14) revealed that an incremental increase in air flow rate caused percentage removal to increase for different liquid loadings. The percentage increase in response was found to be more pronounced at higher liquid loadings. Contrarily, an incremental increase in liquid loading caused percentage removal to decrease for different airflow rates. The percentage decrease in removal fraction decreased at higher airflow rates. Finally, the value of response was found to be greater at higher airflow rates and lower liquid loadings.

Fig. 15 similarly displays the effect of other response (enrichment) with the combined effects of aeration rate and liquid loading at constant dye concentration, 15 ppm. Enrichment was found to decrease substantially with an increase in airflow rate at all liquid loadings. The percentage decrease in response with aeration rate was found to be almost the same irrespective of liquid loading. The liquid loading had a negligible effect on enrichment at various airflow rates. Hence, higher values of enrichment ratios were obtained at lower airflow rates with the negligible effect of liquid loading on the response.

Table 1
Coded and actual levels of three variables

Symbol	Input parameters	Coded levels of variables		
		–1	0	+1
X_1	Air flow rate (mL min^{-1})	150	200	250
X_2	Liquid loading (mL)	600	750	900
X_3	Dye concentration (ppm)	5	15	25

Table 2
Experimental design matrix and response based on the experimental runs proposed by BBD design

Run	Independent variables			Response	
	Air flow rate, X_1 (mL min^{-1})	Liquid loading, X_2 (mL)	Dye concentration, X_3 (ppm)	% Removal	Enrichment ratio
1	250 (+1)	600 (–1)	15 (0)	92.30	3.41
2	200 (0)	600 (–1)	5 (–1)	91.20	4.025
3	200 (0)	600 (–1)	25 (+1)	80.02	4.2
4	200 (0)	900 (+1)	5 (–1)	81.20	3.78
5	250 (+1)	750 (0)	5 (–1)	96.00	1.84
6	150 (–1)	750 (0)	5 (–1)	95.20	7.68
7	250 (+1)	750 (0)	25 (+1)	73.36	2.19
8	200 (0)	900 (+1)	25 (+1)	52.30	4.069
9	200 (0)	750 (0)	15 (0)	74.23	7.35
10	150 (–1)	600 (–1)	15 (0)	71.92	13.8
11	200 (0)	750 (0)	15 (0)	72.01	6.8
12	250 (+1)	900 (+1)	15 (0)	85.00	3.27
13	150 (–1)	900 (+1)	15 (0)	54.34	14.5
14	150 (–1)	750 (0)	25 (+1)	55.20	7.39
15	200 (0)	750 (0)	15 (0)	80.02	8.2

Table 3
Results of ANOVA for the two developed models, percentage removal, and enrichment ratio

		Percentage removal				Enrichment ratio			
Source	df	Adj. SS	Adj. MS	*F*-value	*p*-value	Adj. SS	Adj. MS	*F*-value	*p*-value
Model	9	2,651.18	294.58	5.96	0.032	191.33	21.266	7.03	0.022
Linear	3	2,421.27	807.09	16.33	0.005	133.373	44.458	14.70	0.006
X_1	1	612.50	612.50	12.40	0.017	133.334	133.334	44.10	0.001
X_2	1	489.85	489.85	9.91	0.025	0.004	0.004	0.00	0.972
X_3	1	1,318.92	1,318.92	26.69	0.004	0.034	0.034	0.01	0.919
Square	3	49.65	16.55	0.33	0.802	57.737	19.246	6.37	0.037
X_1^2	1	16.52	16.52	0.33	0.588	3.885	3.885	1.28	0.308
X_2^2	1	9.99	9.99	0.20	0.672	0.268	0.268	0.09	0.778
X_3^2	1	21.36	21.36	0.43	0.540	50.568	50.568	16.73	0.009
2 – Way interaction	3	180.26	60.09	1.22	0.395	0.282	0.094	0.03	0.992
X_1X_2	1	26.42	26.42	0.53	0.497	0.176	0.176	0.06	0.819
X_1X_3	1	75.34	75.34	1.52	0.272	0.102	0.102	0.03	0.861
X_2X_3	1	78.50	78.50	1.59	0.263	0.003	0.003	0.00	0.975
Error	5	247.07	49.41			15.117	3.023		
Lack-of-fit	3	212.87	70.96	4.15	0.200	14.122	4.707	9.46	0.097
Pure error	2	34.20	17.10			0.995	0.497		
Total	14	2,898.25				206.509			

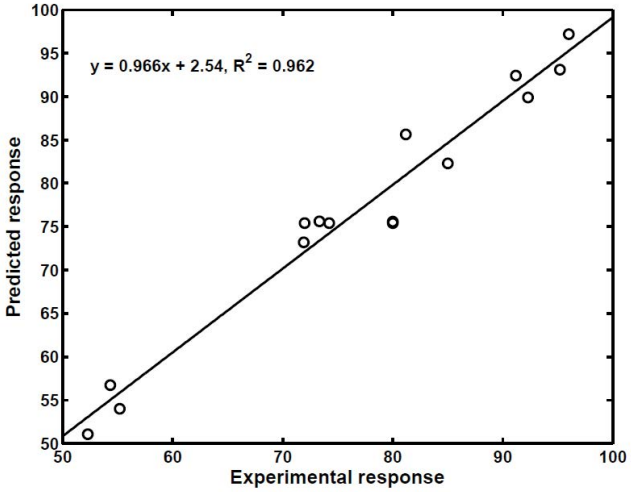

Fig. 10. Linear plot showing comparison between experimental response and predicted response for percentage removal.

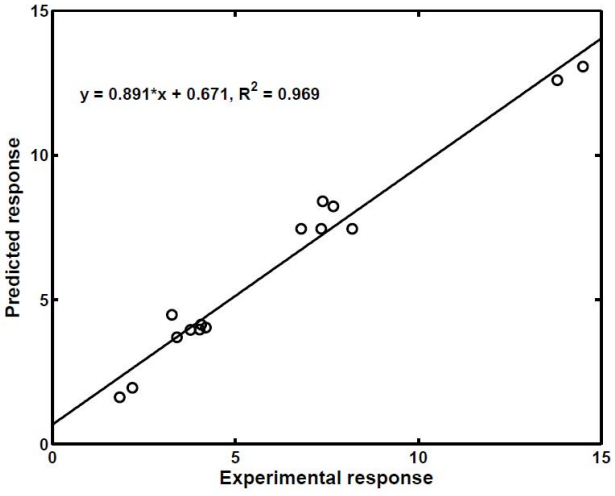

Fig. 11. Linear plot showing comparison between experimental response and predicted response for enrichment ratio.

2.7.3. Interaction effects of airflow rate and dye concentration

Fig. 16 illustrates the interaction effects of aeration rate and dye concentration on percentage removal at a middle value of liquid loading, that is, 750 mL. Fig. 16 divulges that with the incremental increase in aeration rate, the response increases at all values of dye concentration. At low dye concentrations, the percentage increase in the response was found to be less while it increased at higher concentrations. On the other hand, removal fraction decreased with the incremental increase in dye concentration at various airflow rates. The percentage decrease in the response became lesser at higher flow rates. Hence, it can be concluded that higher flow rates and lower dye concentrations would result in more percentage removals.

Similarly, the combined effects of these variables on enrichment ratio were depicted in Fig. 17. The response surface plot indicated a decrease in enrichment ratio at all dye concentrations with an incremental increase in aeration rate. However, the percentage decrease in enrichment ratio was found to be nearly the same at all dye concentrations on varying the airflow rate. The response surface plot also revealed the variation of enrichment ratio at a given flow rate for changing dye concentrations which were found to

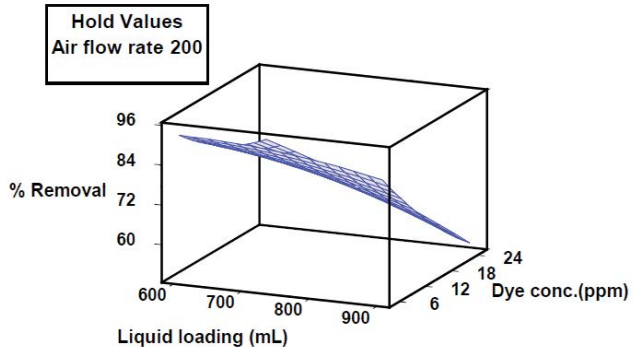

Fig. 12. Response surface plot of percentage removal with liquid loading and dye concentration.

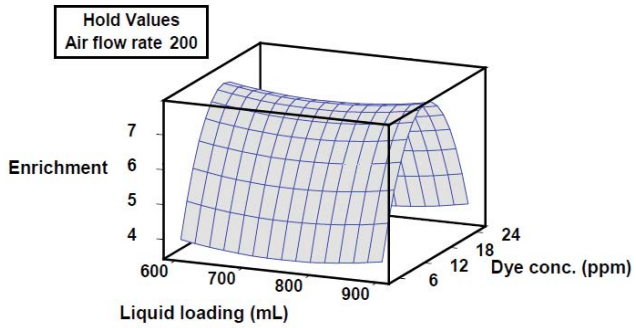

Fig. 13. Response surface plot of enrichment ratio with liquid loading and dye concentration.

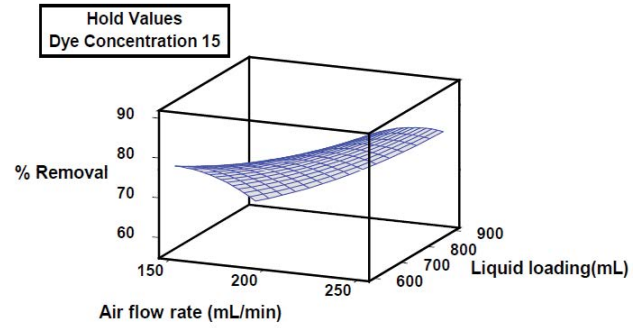

Fig. 14. Response surface plot of percentage removal with air flow rate and liquid loading.

be minimum at 5 ppm, increased to a maximum value, and then fell again. Hence, low airflow rates and intermediate dye concentration favored higher enrichment values.

2.7.4. Multi-objective optimization using GRA

GRA is a tool employed in various fields of engineering for optimization purposes where more than one output or response is involved. In the present problem, this technique has been utilized to maximize both percentage removal and enrichment ratio to find out the optimum values of input variables (air flow rate, liquid loading, and

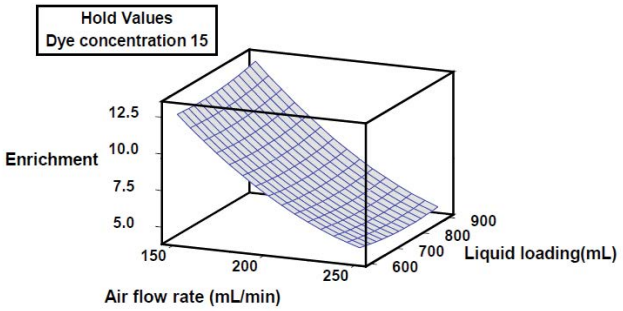

Fig. 15. Response surface plot of enrichment ratio with air flow rate and liquid loading.

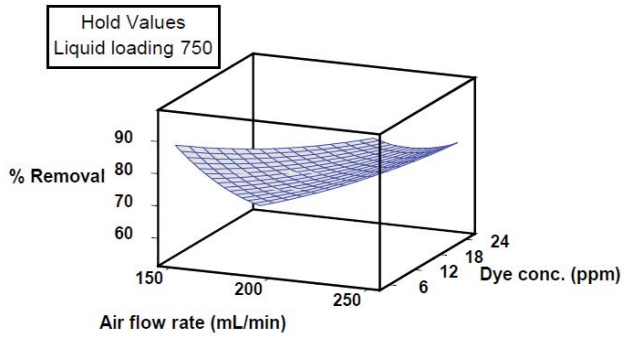

Fig. 16. Response surface plot of percentage removal with air flow rate and dye concentration.

dye concentration). In this technique, the original experimental data was first pre-processed to change the original sequence into a comparable sequence. The purpose of this transformation is simply to avoid any confusion arising due to different units of the responses involved with the process. For this, normalization of data was performed which transformed all the experimental data between 0 and 1, known as grey relational generating. For data normalization, the following equations are used [30]:

Lower is better (LB):

$$X_i^*(k) = \frac{\max X_i(k) - X_i(k)}{\max X_i(k) - \min X_i(k)} \tag{13}$$

Higher is better (HB):

$$X_i^*(k) = \frac{X_i(k) - \min X_i(k)}{\max X_i(k) - \min X_i(k)} \tag{14}$$

Nominal is the best (NB):

$$X_i^* = 1 - \frac{\left|X_i(k) - X_{0b}(k)\right|}{\max X_i(k) - X_{0b}(k)} \tag{15}$$

where $i = 1,2,3\ldots,n$; $k = 1,2,3\ldots, p$; X_i^* is the normalized value in the ith sequence of the kth element; $X_{0b}(k)$ is the desired value of the kth response; $\max X_i(k)$ and $\min X_i(k)$ are the

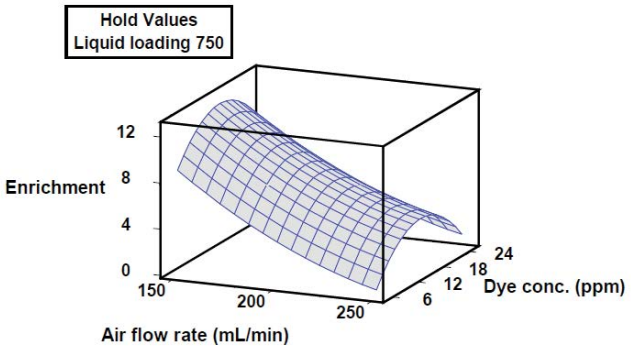

Fig. 17. Response surface plot of enrichment ratio with air flow rate and dye concentration.

maximum and minimum value of the $X_i(k)$, respectively; n and p are the numbers of experiments and responses, respectively.

In this work, as already stated, higher values of both the responses were desired, hence Eq. (14) was utilized for the data normalization.

The grey relational coefficients were then estimated from the following expression:

$$\xi_{0,i}(k)=\frac{\Delta\min+\zeta\cdot\Delta\max}{\Delta_{0,i}(k)+\zeta\cdot\Delta\max},\quad i=1,\ldots,n;\quad k=1,2,\ldots,p \tag{16}$$

where $\xi_{0,i}(k)$ is the relative difference between the kth element of comparative sequence X_i and reference sequence X_0, and $\Delta_{0,i}(k)$ is the difference between the absolute values of $X_0(k)$ and $X_i(k)$.

$$\Delta_{0,i}(k)=\left|X_0^*(k)-X_i^*(k)\right| \tag{17}$$

$$\Delta\max=\max_i\max_k\left|X_0^*(k)-X_i^*(k)\right| \tag{18}$$

$$\Delta\min=\min_i\min_k\left|X_0^*(k)-X_i^*(k)\right| \tag{19}$$

where ζ is the distinguishing coefficient lying between 0 and 1. The ζ value was taken as 0.5 in the subsequent calculations [31].

2.7.5. Weight calculation using the entropy method

The grey relational grade is generally found out by averaging grey relational coefficients. However, the influence of each response to a system may vary while dealing with actual engineering problems. Therefore, weights of all the corresponding responses need to be calculated for the actual representation of the process. Here, the entropy measurement method was employed for the computation of grey relational grade. This entropy concept, when applied to a weight measurement, tells us that an attribute having more entropy tends to have more diversity in responses and thus that attribute is most significant with respect to response. It was proposed as the mapping function f_i: [0,1] → [0,1] and should meet following requirements: (1) $f_i(0) = 0$,(2) $f_i(x) = f_i(1–x)$, (3) $f_i(x)$ is monotonic increasing when $0 < \in < 0.5$ [32]. Hence, for the entropy measurement following function can be used as a mapping function:

$$w_e(x)=xe^{(1-x)}+(1-x)e^x-1 \tag{20}$$

This function attains the maximum value of 0.6478 at $x = 0.5$. Now the entropy function is defined as:

$$W\equiv\frac{1}{\left(e^{0.5}-1\right)n}\sum_{i=1}^{n}w_e(x_i) \tag{21}$$

The step-wise procedure for the entropy measurement of each response is as follows [32]:

- Summation of grey relational coefficient in all sequences for each response:

$$D_j=\sum_{i=1}^{n}\xi_i(j),\qquad j=1,2,\ldots,p. \tag{22}$$

- Normalized coefficient:

$$k=\frac{1}{\left(e^{0.5}-1\right)n}=\frac{1}{0.6487n} \tag{23}$$

- Entropy of each response:

$$e_j=k\sum_{i=1}^{n}w_e\left(\frac{\xi_i(j)}{D_j}\right),\qquad j=1,2,\ldots,p \tag{24}$$

- Total entropy:

$$E=\sum_{j=1}^{p}e_j \tag{25}$$

- Weight of each response

$$w_j=\frac{\frac{1}{p}-E\left[1-e_j\right]}{\sum_{j=1}^{p}\frac{1}{p}-E\left[1-e_j\right]},\qquad i=1,2,\ldots,p \tag{26}$$

Grey relational grade is finally estimated by the expression given by:

$$\Gamma_{0,i}=\sum_{k=1}^{p}w_k\xi_{0,i}(k),\qquad i=1,2,\ldots,n \tag{27}$$

3. Results and discussion

The response (output) of the foam fractionation column for various input variables obtained experimentally (Table 2) were normalized using Eq. (14). The sequences for percentage removal and enrichment ratio are listed in

Table 4 for each experimental run following data pre-processing. Grey relational coefficients for both the responses were first estimated by using Eq. (16) after substituting the values of deviation sequence for each experimental run. The weights of both the percentage removal and enrichment ratio were found to be 0.5025 and 0.4925, respectively, calculated by employing Eq. (26). These weights obtained for each response from entropy measurements were subsequently utilized in estimating grey relational grade by employing Eq. (27), reported in Table 4. The greatest value of grey relational grade in a sequence is indicative of the closest value to the desired value of the response. As observed from Table 4 and Fig. 18, experiment no. 6 which yielded the largest value of grey relational grade (rank no. 1) provided the best performance of foam fractionation column with respect to both percentage removal and enrichment ratio. Table 5 presents the average grey relational grade values at all three levels of the experiment for all three operating variables employed in the experimentation process. The optimum values (largest value out of three levels for each input variable) marked in Table 5 are the best combination of variables to obtain the desired response. Therefore the best combination of operating variables was: volumetric flow rate of air = 150 mL min^{-1}, liquid loading = 600 mL, and dye concentration = 5 ppm; for getting the maximum value of grey relational grade, hence most favorable operating conditions for percentage removal and enrichment ratio. The last column of Table 5 shows the difference between the maximum and minimum value of grey relational grade for all three operating variables. The highest value of 0.20398 was obtained for dye concentration followed by air flow rate and liquid loading. Hence dye concentration was considered as the most influencing parameter with respect to response (percentage removal and enrichment ratio) with liquid loading having the least effect on response. Further, ANOVA was applied to grey relational grade values to ascertain the quantitative contribution of each operating variable on the performance of the foam fractionation column. The following expressions were used for preparing Table 6 [33]:

$$\bar{\gamma} = \frac{1}{13}\sum_{i=1}^{13}\gamma_i, \quad S_T = \sum_{i=1}^{13}\left(\gamma_i - \bar{\gamma}\right)^2, \quad S_A = 3\sum_{q=1}^{3}\left(\gamma_{A_q} - \bar{\gamma}\right)^2,$$
$$S_e = S_T - S_A - S_B - S_C,$$
$$V_A = \frac{S_A}{f_A}, F_A = \frac{V_A}{V_e}, \quad \mathrm{PC}(\%) = \frac{S_A}{S_T}\times 100 \tag{28}$$

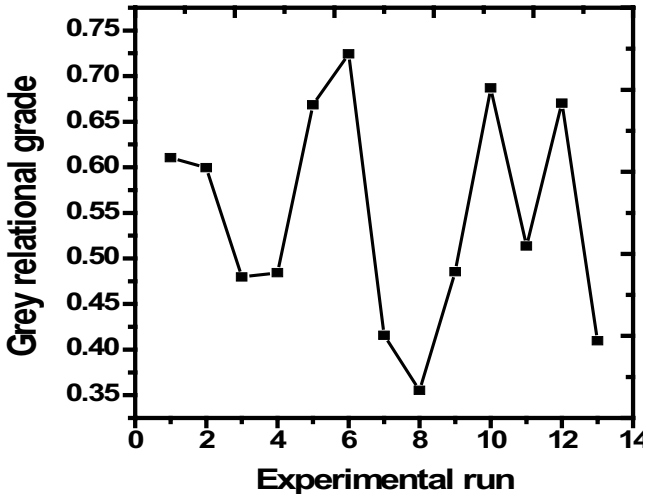

Fig. 18. Variation of grey relational grade with experimental run.

Table 4
Sequences of each response after data pre-processing, grey relational coefficient (GRC), grey relational grade (GRG), and rank of each experiment

Experimental Run	Normalized sequences		Deviation sequences		GRC		GRG	Rank
	% R^a	E^b	% R^a	E^b	% R^a	E^b		
1.	0.9153318	0.124013	0.084668	0.875987	0.855186	0.363375	0.61051	5
2.	0.8901602	0.172591	0.10984	0.827409	0.819887	0.376674	0.599389	6
3.	0.6343249	0.186414	0.365675	0.813586	0.577584	0.380637	0.479603	10
4.	0.6613272	0.153239	0.338673	0.846761	0.59618	0.371261	0.484283	9
5.	1	0	0	1	1	0.333333	0.668333	4
6.	0.9816934	0.461295	0.018307	0.538705	0.96468	0.481369	0.724233	1
7.	0.4819222	0.027646	0.518078	0.972354	0.491122	0.339592	0.415736	11
8.	0	0.176066	1	0.823934	0.333333	0.377662	0.355387	13
9.	0.5018307	0.435229	0.498169	0.564771	0.500917	0.469585	0.485329	8
10.	0.4489703	0.944708	0.55103	0.055292	0.475724	0.900427	0.687014	2
11.	0.7482838	0.112954	0.251716	0.887046	0.665145	0.360478	0.513573	7
12.	0.0466819	1	0.953318	0	0.34404	1	0.67038	3
13.	0.0663616	0.438389	0.933638	0.561611	0.348763	0.470982	0.409567	12

[a]Percentage removal;
[b]Enrichment ratio.

where $\bar{\gamma}$ is the mean of grey relational grades, S_T is the sum of squares of the variance between γ_i and $\bar{\gamma}$, S_A is the sum of squares of the variance between each level of airflow rate and $\bar{\gamma}$, similarly, S_B and S_C were calculated for liquid loading and dye concentration, q is the qth level of the input variable, S_e is the error between S_T and the sum of squares of the variance of all input variables, f_A is the degrees of freedom for airflow rate, V_A is the variance for airflow rate, F_A is the F-test value for airflow rate, and PC is the percentage contribution of airflow rate.

The percentage contribution in descending order (Table 6) was found to be: dye concentration 63.65%, airflow rate 26.17%, and liquid loading 10.16%; toward response. Finally, we concluded that dye concentration had the strongest effect on percentage removal and enrichment among all input parameters investigated.

3.1. Confirmation tests

Next, confirmation tests were carried out to substantiate the fact that foam fractionation column operated at optimum conditions would yield maximum grey relational grade value. The expected value of grey relational grade (γ_e) can be estimated at these optimum conditions by using the following expression:

$$\gamma_e = \overline{\gamma} + \sum_{i=1}^{p}\left(\overline{\gamma}_i - \overline{\gamma}\right) \tag{29}$$

where $\bar{\gamma}_i$ is mean grey relational grade value at the optimum level and p is the number of input variables. Table 7 lists the results of confirmation experiments where improvement in the grey relational grade value is visible in comparison to the value obtained from experiment no. 6 (Table 4). Finally, the percentage removal of 95.8 and enrichment ratio of 7.7 was obtained at these optimum conditions.

4. Conclusions

The present study dealt with the removal of MB using SDS as a collector. SDS concentration of 500 ppm and initial pH near 7 were found to be the optimum conditions for the isolation of MB. At these optimized conditions, the effect of operating variables like aeration rate (150–250 mL min^{-1}), liquid loading (600–900 mL), and dye concentration (5–25 ppm) on percentage removal, enrichment ratio, and surface excess were investigated. Following conclusions were drawn from these experimental studies:

- Percentage removal increased, enrichment ratio decreased, and surface excess decreased with an increase in aeration rate.
- Percentage removal decreased, enrichment ratio remained almost constant, and surface excess increased with an increase in liquid loading.
- Percentage removal declined with the rise in dye concentration while enrichment ratio and surface excess initially increased and then reduced with an increase in dye concentration.

Further, the RSM technique was successfully applied to develop a mathematical model and to investigate the interaction effect between airflow rate, liquid loading, and dye concentration on percentage removal and enrichment ratio. Results of ANOVA demonstrated the significance of the polynomial regression model ($P < 0.05$), also higher values of R^2 (0.962 for percentage removal and 0.969 for

Table 5
Response table for the grey relational grade

Symbol	Input parameters	Average grey relational grade			
		Level 1	Level 2	Level 3	Max.–Min.
X_1	Air flow rate	0.622798[a]	0.480798	0.55204	0.142000251
X_2	Liquid loading	0.594129[a]	0.54064	0.50591	0.088223016
X_3	Dye concentration	0.619059[a]	0.593361	0.41507	0.203986127

[a]Optimum value.

Table 6
Results of ANOVA for grey relational grade

Symbol	Input parameters	Degrees of freedom (f)	Sum of squares (S)	Variance (V)	F-ratio (F)	PC[a] (%)
X_1	Air flow rate	2	0.03051	0.015255	1.59	26.17
X_2	Liquid loading	2	0.01185	0.005925	0.62	10.16
X_3	Dye concentration	2	0.07419	0.037095	3.87	63.65
Error		6	0.057413	0.009568	–	–
Total		12	0.173963			100

[a]Percentage contribution

Table 7
Results of confirmation experiment

	Optimal operating variables	
	Prediction	Experiment
Level	$X_{1_1} X_{2_1} X_{3_1}$	$X_{1_1} X_{2_1} X_{3_1}$
% Removal	–	95.8
Enrichment ratio	–	7.7
Grey relational grade	0.743164	0.737742

enrichment ratio) affirmed the validity of the polynomial equation. Finally, the GRA was performed to ascertain the optimum values of operating variables with an objective to maximize both percentage removal and enrichment ratio simultaneously. Optimum values of operating variables were found to be: 150 mL min^{-1} air flow rate, 600 mL liquid loading, and 5 ppm dye concentration; which gave percentage removal of 95.8 and enrichment ratio of 7.7.

References

[1] S. Valliammai, Y. Subbareddy, K.S. Nagaraja, B. Jeyaraj, Removal of methylene blue from aqueous solution by activated carbon of *Vigna Mungo* L and *Paspalum scrobiculatum*: equilibrium, kinetics and thermodynamic studies, Indian J. Chem. Technol., 24 (2017) 134–144.

[2] V.K. Gupta, R. Kumar, A. Nayak, T.A. Saleh, M.A. Barakat, Adsorptive removal of dyes from aqueous solution onto carbon nanotubes: a review, Adv. Colloid Interface Sci., 193–194 (2013) 24–34.

[3] A. Salima, B. Benaouda, B. Noureddine, L. Duclaux, Application of ulva lactuca and systoceira stricta algae-based activated carbons to hazardous cationic dyes removal from industrial effluents, Water Res., 47 (2013) 3375–3388.

[4] M.R. Gadekar, M.M. Ahammed, Modelling dye removal by adsorption onto water treatment residuals using combined response surface methodology-artificial neural network approach, J. Environ. Manage., 231 (2019) 241–248.

[5] K. Karthick, C. Namasivayam, L.M. Pragasan, Removal of direct red 12B from aqueous medium by ZnCl2 activated Jatropha husk carbon: adsorption dynamics and equilibrium studies, Indian J. Chem. Technol., 24 (2017) 73–81.

[6] C.S. Oliveira, C. Airoldi, Pyridine derivative covalently bonded on chitoasan pendant chains for textile dye removal, Carbohydr. Polym., 102 (2014) 38–46.

[7] W.G. Kuo, Decolorizing dye wastewater with Fenton's reagent, Water Res., 26 (1992) 881–886.

[8] H.M.H. Gad, A.A. El-Sayed, Activated carbon from agricultural by-products for the removal of Rhodamine-B from aqueous solution, J. Hazard. Mater., 168 (2009) 1070–1081.

[9] F.A. Pavan, S.L.P. Dias, E.C. Lima, E.V. Benvenutti, Removal of Congo Red from aqueous solution by anilinepropylsilica xerogel, Dyes Pigm., 76 (2008) 64–69.

[10] K.A.G. Gusmao, L.V.A. Gurgel, T.M.S. Melo, L.F. Gil, Application of succinylated sugarcane bagasse as adsorbent to remove methylene blue and gentian violet from aqueous solutions–kinetic and equilibrium studies, Dyes Pigm., 92 (2012) 967–974.

[11] A. Mittal, J. Mittal, A. Malviya, V.K. Gupta, Adsorptive removal of hazardous anionic dye "Congo red" from wastewater using waste materials and recovery by desorption, J. Colloid Interface Sci., 340 (2009) 16–26.

[12] I. Arslan-Alaton, B.H. Gursoy, J.E. Schimdt, Advanced oxidation of acid and reactive dyes: effect of Fenton treatment on aerobic, anoxic and anaerobic processes, Dyes Pigm., 78 (2008) 117–130.

[13] W.S. Chang, H.T. Tran, D.H. Park, R.H. Zhang, D.H. Ahn, Ammonium nitrogen removal characteristics of zeolite media in a biological aerated filter (BAF) for the treatment of textile wastewater, J. Ind. Eng. Chem., 15 (2009) 524–528.

[14] J.P. Jadhav, G.K. Parshetti, S.D. Kalme, S.P. Govindwar, Decolourization of azo dye methyl red by *Saccharomyces cerevisiae* MTCC 463, Chemosphere, 68 (2007) 394–400.

[15] I.D. Kamalanathan, P.J. Martin, Competitive adsorption of surfactant–protein mixtures in a continuous stripping mode foam fractionation column, Chem. Eng. Sci., 146 (2016) 291–301.

[16] B. Burghoff, Foam fractionation applications, J. Biotechnol., 161 (2012) 126–137.

[17] R. Lemlich, Adsorptive bubble separation methods—foam fractionation and allied techniques, Ind. Eng. Chem., 60 (1968) 16–29.

[18] Z. Zhang, Z. Wu, G. Liu, Interfacial adsorption of methyl orange in liquid phase of foam fractionation using dodecyl dimethyl betaine as the collector, J. Ind. Eng. Chem., 28 (2015) 184–189.

[19] X. Fei, W. Li, S. Zhu, L. Liu, Y. Yang, Simultaneous treatment of dye wastewater and surfactant wastewater by foam separation: experimental and mesoscopic simulation study, Sep. Sci. Technol., 53 (2017) 1604–1610.

[20] K. Lu, X.L. Zhang, Y.L. Zhao, Z.L. Wu, Removal of color from textile dyeing wastewater by foam fractionation, J. Hazard. Mater., 182 (2010) 928–932.

[21] D. Zhang, G. Zeng, J. Huang, W. Bi, X. Gengxin, Spectroscopic studies of dye-surfactant interactions with the co-existence of heavy metal ions for foam fractionation, J. Environ. Sci., 24 (2012) 2068–2074.

[22] K. Lu, R. Li, Z. Wu, K. Hou, X. Du, Y. Zhao, Wall effect on rising foam drainage and its application to foam separation, Sep. Purif. Technol., 118 (2013) 710–715.

[23] B.Y. Tak, B.S. Tak, Y.J. Kim, Y.J. Park, Y.H. Yoon, G.H. Min, Optimization of color and COD removal from livestock wastewater by electrocoagulation process: application of Box-Behnken design (BBD), J. Ind. Eng. Chem., 28 (2015) 307–315.

[24] C. Liyana-Pathirana, F. Shahidi, Optimization of extraction of phenolic compounds from wheat using response surface methodology, Food Chem., 93 (2005) 47–56.

[25] E. Kiassos, S. Mylonaki, D.P. Makris, P. Kefalas, Implementation of response surface methodology to optimize extraction of onion (*Allium cepa*) solid waste phenolics, Innovation Food Sci. Emerg. Technol., 10 (2009) 246–252.

[26] S. Sharma, N.N. Dutta, G.K. Agrawal, Optimization of copper extraction from spent LTS catalyst ($CuO–ZnO–Al_2O_3$) using chelating agent: Box-behnken experimental design methodology, Russ. J. Nonferrous Met., 58 (2017) 22–29.

[27] R.H. Myers, D.C. Mongtgomery, C.M. Anderson-Cook, Response Surface Methodology: Process and Product Optimization Using Designed Experiments, Wiley, New York, NY, 2009.

[28] H.R. Fouladian, M. Behbahani, Solid phase extraction of Pb(II) and Cd(II) in food, soil, and water samples based on 1-(2-pyridylazo)-2-naphthol-functionalized organic-inorganic mesoporous material with the aid of experimental design methodology, Food Anal. Methods, 8 (2015) 982–993.

[29] A.A. Patil, S.S. Bhusari, D.B. Shinde, P.S. Wakte, Optimization of process variables for phyllanthin extraction from *Phyllanthus amarus* leaves by supercritical fluid using a Box–Behnken experimental design followed by HPLC identification, Acta Pharm., 63 (2013) 193–207.

[30] A. Sharma, V. Yadava, Optimization of cut quality characteristics during Nd: YAG laser straight cutting of Ni-based superalloy thin sheet using grey relational analysis with entropy measurement, Mater. Manuf. Processes, 26 (2011) 1522–1529.

[31] N. Tosun, Determination of optimum parameters for multi-performance characteristics in drilling by using grey relational analysis, Int. J. Adv. Manuf. Technol., 28 (2006) 450–455.

[32] K.T. Wen, T.C. Chang, M.L. You, The grey entropy and its application in weighting analysis, IEEE Int. Conf. Syst. Man Cybernet., 2 (1998), 1842–1844 doi: 10.1109/ICSMC.1998.728163.

[33] M.J. Tsai, C.H. Li, The use of grey relational analysis to determine laser cutting parameters for QFN packages with multiple performance characteristics, Opt. Laser Technol., 41 (2009) 914–921.